



## Prediction of the shock arrival time with SEP observations

G. Qin,<sup>1</sup> M. Zhang,<sup>2</sup> and H. K. Rassoul<sup>2</sup>

Received 6 April 2009; revised 21 June 2009; accepted 6 July 2009; published 16 September 2009.

[1] Real-time prediction of the arrival times at Earth of shocks is very important for space weather research. Recently, various models for shock propagation are used to forecast the shock arriving times (SATs) with information of initial coronal shock and flare from near real-time radio and X-ray data. In this paper, we add the use of solar energetic particles (SEP) observation to improve the shock arrival time (SAT) prediction. High-energy SEPs originating from flares move to the Earth much faster than the shocks related to the same flares. We develop an SAT prediction model by combining a well-known shock propagation model, STOA, and the analysis of SEPs detected at Earth. We demonstrate that the SAT predictions are improved by the new model with the help of 38–53 keV electron SEP observations. In particular, the correct prediction to false alarm ratio is improved significantly.

**Citation:** Qin, G., M. Zhang, and H. K. Rassoul (2009), Prediction of the shock arrival time with SEP observations, *J. Geophys. Res.*, 114, A09104, doi:10.1029/2009JA014332.

### 1. Introduction

[2] The arrival of interplanetary shocks can change the terrestrial environment very much and have strong space weather effects. Therefore real-time prediction of shock arrivals at Earth is very important for the study of space weather. Various physics-based models for shock propagation have been developed. The shock time of arrival (STOA) model is based on modified similarity theory of blast waves with the piston-driving concept [Dryer and Smart, 1984; Smart *et al.*, 1984, 1986; Smart and Shea, 1985; Lewis and Dryer, 1987]. The interplanetary shock propagation model (ISPM) is based on a 2.5-D MHD parametric study of simulated shocks [Smith and Dryer, 1990]. The hakamada-Akasofu-Fry version 2 (HAFv.2) model is a modified kinematic model that concentrates on the time and location variation of solar wind speed, density, magnetic field, and dynamic pressure [Fry *et al.*, 2001]. Recently the forecast capability of the models has been evaluated against flare-related shock observations with information of initial shock and flare from near real-time radio and X-ray data [e.g., Smith *et al.*, 2000, 2004a, 2009; Fry *et al.*, 2003; McKenna-Lawlor *et al.*, 2006], the results show that the prediction skill of all these models is essentially the same, and that their success rates are usually not very high. Therefore it is very important for us to find ways to improve the prediction of the models.

[3] Alternative SAT prediction models have also been developed based on different methods, e.g., initial CME speed [Manoharan *et al.*, 2004], lateral expansion CME speed [Schwenn *et al.*, 2005], and analytical study for blast

wave propagation with the energy estimation method in the ISPM model [Feng and Zhao, 2006]. In addition, Feng *et al.* [2009] developed a database method for prediction of SATs at Earth by creating databases using previous numerical prediction models that consider initial shock speed and source longitude's impact. Thus with the input parameters, such as source conditions and the time of the observed solar events, the SAT may be obtained immediately by looking up the databases. It is also demonstrated that the prediction performance of the database model is similar to that of the previous methods.

[4] It is believed that strong solar flares play an important physical role in the generation of CMEs, which, if energetic enough, can drive interplanetary shocks [Dryer, 1996, and references therein]. In other words, the complex physical process from which these interplanetary shocks originate may also give rise to flares. Therefore among other inputs, information of flares should be included in models to predict SATs. Since flares and interplanetary shocks generated by flares and CMEs can produce SEP protons and electrons, it is also useful to include SEP measurements in SAT prediction models.

[5] Smith and coworkers [Smith and Zwickl, 1999; Smith *et al.*, 2004b] used low-energy SEP observations to predict the magnitudes of postshock geomagnetic disturbances based on the fact that low-energy energetic ion enhancements are mainly caused by acceleration by interplanetary shocks. Recently, Lam [2009] studied operational geomagnetic disturbance forecasting with the help of low-energy energetic particle (electron and proton) observations. Since very high-energy solar energetic particles (SEPs), e.g., high-energy solar electrons, are considered to be accelerated by flares, such kinds of SEPs can be associated with interplanetary shocks related to the same flare, in other words, these SEPs are signatures of flare-related shocks. Furthermore, as these SEPs move to Earth much faster than the shocks, it is possible to improve the real-time predictions of SATs of shock

<sup>1</sup>State Key Laboratory of Space Weather, Center for Space Science and Applied Research, Chinese Academy of Sciences, Beijing, China.

<sup>2</sup>Department of Physics and Space Sciences, Florida Institute of Technology, Melbourne, Florida, USA.

propagation models with the help of the analysis of very high-energy SEPs detected at L1. Theoretically, we can use either high-energy ions or electrons to predict shock arrivals; however, in this work we use electrons since they give earliest warning or longest lead time.

[6] In this paper, we present an SAT prediction method by combining a shock propagation model, STOA, and analysis of high energy, 38–53 keV electron, SEPs detected at L1. In section 2, we describe the STOA model. In section 3, we discuss the SEP measurements to help the prediction of SATs with new models. In section 4, we study the prediction skills of SATs at 1 AU with the models. The conclusions are presented in section 5.

## 2. Description of the STOA Model

[7] In order to predict whether a solar event caused shock can reach the Earth and, if so, the time of arrival of the shock, a various models to simulate the propagation of interplanetary disturbances were developed. Among the models, the shock time of arrival (STOA) model [e.g., *Smart and Shea*, 1985] is widely used. STOA is based on the following assumptions. The initial shock is driven for some time  $\tau$  at the type II speed  $v_{s0}$  for some distance  $v_{s0}\tau$  from the sun, so the shock position at the end of the driven phase is  $r_0 = r_{00} + v_{s0}\tau$ , where  $r_{00}$  is the initial shock position which can be assumed as 1.5 solar radii. After the driven stage, the shock is changed to a blast wave riding over the solar wind speed  $v_{sw}$ . It is further assumed that after the shock converts to a blast wave, the velocity of the shock  $v_s$  measured at any central angular distance  $\theta$  has the form

$$v_s = v_{s0}(\cos \theta + 1)/2. \quad (1)$$

where  $\theta$  can be rewritten as  $\cos \theta = \cos \theta_s \cos \phi_s$  with heliospheric longitude distance  $\theta_s$  and latitude distance  $\phi_s$  [e.g., see *Zhao et al.*, 2007].

[8] As the blast wave propagates through the interplanetary medium, the speed of the shock front  $v_{sr}$  is assumed to be proportional to  $1/\sqrt{r}$ , so we have

$$v_{sr} = \sqrt{\frac{r_0}{r}} v_s. \quad (2)$$

In order to calculate the shock's transit time to a certain location of the solar distance  $r_d$ , the average shock front speed  $v_{avr}$  can be calculated by

$$v_{avr} = \frac{1}{r_d} \int_{r_0}^{r_d} v_{sr} dr = 2v_s \left( \sqrt{\frac{r_0}{r_d}} - \frac{r_0}{r_d} \right) \quad (3)$$

Furthermore, the transit time  $\Delta t$  of the blast wave is written as

$$\Delta t = \frac{r_d}{v_{avr} + v_{sw}}, \quad (4)$$

where  $r_0 \ll r_d$  is used.

[9] STOA model computes the shock magnetoacoustic Mach number  $M_a$  as a measure of the shock strength as

following [e.g., *Smith et al.*, 2000].  $M_a$  is the ratio of the shock

$$M_a = \frac{v_{sr}}{\sqrt{a^2 + V_a^2}}, \quad (5)$$

where  $a$  is sound speed and  $V_a$  is the Alfvén speed. Here the sound speed and Alfvén speed are obtained by assuming a representative solar wind property, proton density,  $n = 5 \text{ cm}^{-3}$ , proton temperature  $T = 10^5 \text{ K}$ , IMF magnitude  $B = 5 \text{ nT}$ , and the adiabatic index  $\gamma = 5/3$ .  $M_a = 1.0$  is a limit below which shocks decay to MHD waves.

## 3. SEP Measurements to Help the Prediction of SATs: New Models STSEP and STOASEP

[10] We can use measurements of SEP at L1 to help the prediction of SATs. Generally we are able to use solar events observation as initial condition to compute SEP flux by numerically solving SEP transport equation [*Parker*, 1963, 1965; *Ng and Wong*, 1979; *Schlüter*, 1985; *Ruffolo*, 1991; *Kocharov et al.*, 1998; *Qin et al.*, 2004, 2005, 2006; *Zhang et al.*, 2009]. If we actually detect SEP flux matching the calculated results, we forecast a shock to arrive at the time calculated by some model, e.g., STOA. Otherwise, we forecast the shock will not arrive. However, it is currently difficult to accurately determine from solar observations the conditions that affect the SEP event. Therefore we use a simple method instead as described below to include the SEP measurements to determine the arrival of shocks.

[11] If we assume the first solar energetic particles with energy  $E$  arriving at L1 move along the Parker interplanetary magnetic field line without scattering or acceleration in interplanetary space, the transit time for these particles to arrive can be written as  $t_f = S_{L1}/v$ . Here,  $v$  is particles speed and  $S_{L1}$  is the length of Parker field line from Sun to L1. For simplicity, we take it as a constant, 1.2 AU. If we use a channel of solar particles data with energy range  $[E_1 : E_2]$ , the transit time of first arriving particles for maximum and minimum of the energy range is in the range  $[t_{f2} : t_{f1}]$ , with  $t_{f1}$  and  $t_{f2}$  being associated with energy  $E_1$  and  $E_2$ , respectively. We use  $F_b$  for the SEP background flux at the time of the solar event  $T_{SE}$ . We also use the average flux  $F_t$  in the time range  $[T_{d0} : T_{d1}]$  as a target flux. Here  $T_{d0}, T_{d1} > T_{SE} + t_{f1}$ , to be defined later.  $F_t$  can be considered as the flux associated with the solar event since  $[T_{d0} : T_{d1}]$  is the time range when the majority of particles in the channel associated with the event arrive at L1. Therefore we have to set  $T_{d0}$  a value larger than  $T_{SE} + t_{f1}$  since the majority of those particles arrive later than the first arriving particles because of scatterings along interplanetary field lines. If the ratio of the target flux and the background flux,  $F_t/F_b$ , is larger than the threshold value  $R$ , the SEPs associated with the solar event are considered detected, therefore, we forecast that a shock will arrive and its time of arrival.

[12] In this article we use 5-min averaged solar energetic electron measurements from the DE1 channel of ACE/EPAM level two data within the range  $[E_1 : E_2] = [38 : 53] \text{ keV}$  [*Gold et al.*, 1998]. The transit time of first arriving particles with energy  $E_1$  and  $E_2$  are  $t_{f1} = 27.33 \text{ min}$  and  $t_{f2} = 23.64 \text{ min}$ , respectively. In order to forecast the shock arrival time

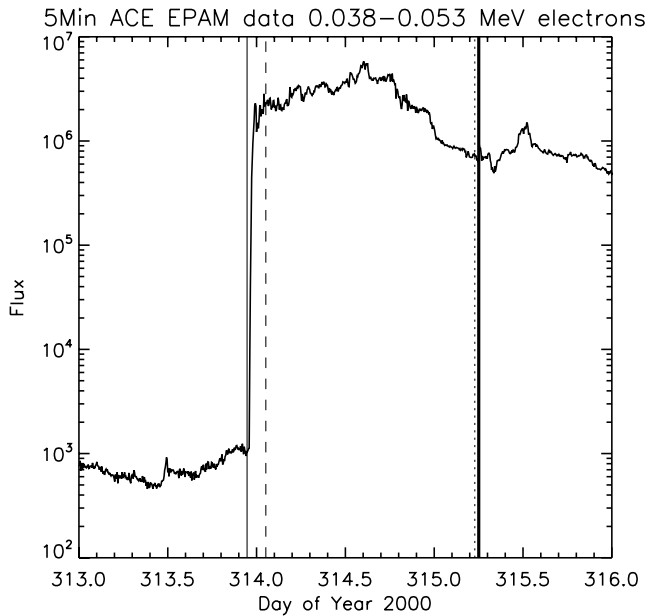


**Figure 1.** Five-minute averaged 38–53 keV electrons flux measured by ACE/EPAM instruments. The thin vertical line indicates the time of a solar event. The dashed line indicates the time at which the decision is made whether the shock will arrive at the Earth by checking the SEP flux with the model STSEP. The dotted line indicates the shock arrival time (SAT) predicted by the model. The thick line indicates the observed SAT.

at Earth, we make the following assumptions. To get the averaged flux, or the target flux  $F_t$ , we take  $T_{d0} = T_{SE} + 142.5$  min and  $T_{d1} = T_{SE} + 152.5$  min to make sure enough data of the flux associated with the solar event can be detected, at the same time to keeping the early warning time. In other words, about 2.5 hours after the solar event, we forecast whether or not the shock will reach Earth.

[13] The background flux,  $F_b$ , is measured in 30-min averages during the time range  $[t_{SE} - 15 \text{ min} : t_{SE} + 15 \text{ min}]$ . Usually, if we choose the threshold value  $R$  to be larger, we can get better prediction results for those shocks that do not reach L1 but get worse prediction results for those shocks that do reach L1, and vice versa. So we have to use an appropriate  $R$ , which here is 1.05, to balance between the two kinds of probability. If we detect SEP associated with the solar event, we forecast that the shock will actually reach the Earth at the arrival time predicted by STOA. We call the new combined model, STSEP.

[14] In the following, we give an example to show how we predict the SAT with this method. Figure 1 shows time profile of the electron flux data from ACE/EPAM instrument as described above. The vertical thin line in Figure 1 indicates the time of the solar event with flare number 2 from observation collected by *McKenna-Lawlor et al.* [2006]. 15 min after this time, the background flux  $F_b$  is determined. The vertical dashed line indicates the time  $T_{d1}$  when the target flux,  $F_t$ , is obtained, and thus the ratio  $F_t/F_b$ . Since the ratio is larger than the threshold value  $R$  we choose, at the time  $T_{d1}$  we forecast that the shock will arrive at L1 with the shock arrival time, indicated by the vertical

dotted line, that was predicted by STOA. The vertical thick line indicates the actual SAT observed by spacecraft at L1. Since the difference between the SAT predicted by the combined model STSEP and that observed by spacecraft is small enough, we consider the prediction as a “hit”.

[15] STOA tends to forecast “too much”, i.e., to forecast the SAT for many events without actual shock arrival at L1 [e.g., *McKenna-Lawlor et al.*, 2006]. On the other hand, we find that our new STSEP model tends to forecast fewer shocks, and therefore, to predict that the shocks will not arrive for some events for which actual shocks arrive at L1 (see results below). Figure 2 shows the scattered plot between the ratio of target SEP flux to the background one,  $F_t/F_b$ , and the predicted interplanetary magnetoacoustic Mach number,  $M_a$ , for the 207 solar events during the maximum phase of Solar Cycle 23 collected by *McKenna-Lawlor et al.* [2006]. To make Figure 2 compact, for events with  $F_t/F_b > 5$  and  $M_a > 5$ , we plot them at  $F_t/F_b = 5$  and  $M_a = 5$ , respectively. Red circles indicate the solar events with observed shock arrival at L1, while green crosses indicate those without. To associate solar events and interplanetary shocks, we use a model STOASEP explained below. From Figure 2 we can see, generally, that the solar events with observed shock arrival at L1 have larger spacecraft measurements of  $F_t/F_b$  or larger predicted  $M_a$  at L1. However, a large proportion of solar events with large  $F_t/F_b$  or  $M_a$ , are not followed by shock arrivals at L1. Using  $M_a$  or  $F_t/F_b$  criteria to predict SAT separately would always give many false alarms or misses.

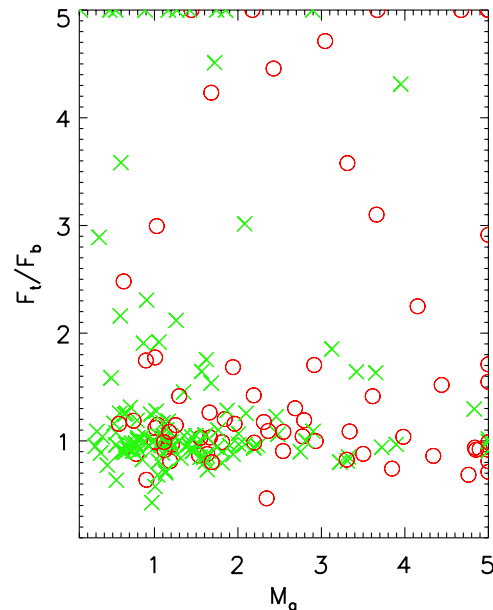


**Figure 2.** Scattered plot between the ratio of target SEP flux to the background one,  $F_t/F_b$ , as defined in the text and the predicted interplanetary disturbance magnetoacoustic Mach number,  $M_a$ , for the 207 solar events during the maximum phase of Solar Cycle 23 collected by *McKenna-Lawlor et al.* [2006]. Events with  $F_t/F_b > 5$  and  $M_a > 5$  are plotted at  $F_t/F_b = 5$  and  $M_a = 5$ , respectively. Red circles indicate the solar events with an observed shock arrival at L1, while green crosses indicate events without following shocks.

**Table 1.** Comparison of the Results Obtained Using Different Models for Samples During the Maximum and Rise Phases of Solar Cycle 23 and for the Composite Sample (Hit Window Size  $\pm 24$  Hours)

Status	Number of Events	Model	(h)	(fa)	(cn)	(m)	(h/m)	(sr)	$\chi^2$	P Value
Cycle max	207	STOA	58	83	48	18	3.2	51	3.71	0.054 <sup>b</sup>
		STSEP	42	47	84	34	1.2	61	7.37	0.007 <sup>a</sup>
		STOASEP	49	47	84	27	1.8	64	15.8	<0.001 <sup>a</sup>
Cycle rise	170	STOA	50	56	49	15	3.3	58	9.52	0.002 <sup>a</sup>
		STSEP	34	48	57	31	1.1	54	0.70	0.4
		STOASEP	44	35	70	21	2.1	67	19.1	<0.001 <sup>a</sup>
Composite	377	STOA	108	139	97	33	3.3	54	12.2	<0.001 <sup>a</sup>
		STSEP	76	95	141	65	1.2	58	6.63	0.01 <sup>a</sup>
		STOASEP	93	82	154	48	1.9	66	34.6	<0.001 <sup>a</sup>

<sup>a</sup>High level of significance with  $p < 0.05$ .

<sup>b</sup>Lesser, but still acceptable, level significance with  $0.05 < p < 0.2$ .

[16] We get a better model using the magnetoacoustic Mach number  $M_a$  criteria and SEP detection criteria together to decide if the shock will actually arrive at the L1. For example, we assume that we can forecast that the shock will reach the Earth only when the predicted  $M_a$  at L1 is larger than 1 and the SEP associated with the solar event is detected. We also consider the possibility that, in some cases, the solar energetic particles associated with the solar events might be masked by some interplanetary local effects so that they would not be detected. Furthermore, we are usually more confident that the shock will arrive if the magnetoacoustic Mach number  $M_a$  is larger (see Figure 2). Therefore we also forecast that, if  $M_a \geq 2$ , the shock will reach L1 no matter whether or not the SEP associated with the solar event is detected. The new model considering both SEP and  $M_a$  is called STOASEP.

#### 4. Prediction at 1 AU

[17] In order to evaluate these two new models using SEP measurements, we study 170 events data during the rise phase of Solar Cycle 23 compiled by *Fry et al.* [2003] and 207 events data during the maximum phase of the solar cycle compiled by *McKenna-Lawlor et al.* [2006], which spans the period of 4 September 1997–3 August 2002.

[18] As described by *Smith et al.* [2004a], we search for shocks within a window of approximately one to five days following the solar events in order to make associations of the solar flare with interplanetary shocks. For any model, if a shock is predicted and observed within the  $\pm 24$  hours, we consider the prediction a ‘‘Hit’’ (h). If no shock is predicted and none is observed in the 4-day window following the solar event, we consider it as ‘‘Correct Null’’ (cn). If a shock is observed but no shock is predicted within  $\pm 24$  hours, we consider it as ‘‘Miss’’ (m). If a shock is predicted but none is observed within the 4-day window, we consider it as ‘‘False alarm’’ (fa).

[19] Table 1 shows the performance of the three models (STOA, STSEP, and STOASEP) with window size of  $\pm 24$  hours. Note that the association of solar events and shock arrivals for each model is slightly different in order to obtain best success rate and root mean square of  $\Delta T$  (see below). The top section of Table 1 is the result of analysis on the 207 events during the maximum phase of Solar Cycle 23 collected by *McKenna-Lawlor et al.* [2006], the middle one is for 170 events during the rise phase of the

cycle collected by *Fry et al.* [2003], while the bottom one is for the total 377 events including both of the two phases above. In the table, columns 4–7 show contingency entries; column 8 shows associated hit/miss ratios (h/m); and column 9 shows corresponding success rates (sr) of the models. In order to indicate a dependency between the SAT at L1 and their prediction by different models, we apply a  $\chi^2$  test to the predictions with the results,  $\chi^2$  and  $p$  values, shown in columns 10 and 11. Here we use a significance level by a  $p$  value of 0.05 and a lesser level of significance while still acceptable by a  $p$  value of 0.05–0.2, marked by ‘a’ and ‘b’ in column 11, respectively, following *McKenna-Lawlor et al.* [2006].

[20] From the Table 1 we can see, during solar maximum, the success rates for STOA, STSEP, and STOASEP are 51%, 61%, and 64%, respectively, i.e., the success rates for STSEP and STOASEP are better than that for STOA. However, during the rising time for the same cycle, the success rates for STOA, STSEP, and STOASEP are 58%, 54%, and 67%, respectively, the success rate for STOASEP is better than that for STSEP and STOA. Table 1 also shows that STOA has the highest number of hits (h), false alarm (fa), the ratio of hits to misses (h/m), and the lowest correct null (cn) and misses (m). This is because STOA tends to predict more shocks than the other two models resulting in higher number of hits and false alarms. On the other hand, STSEP and STOASEP have the lower hits, false alarms, h/m, and higher correct null and misses since they tend to predict fewer shocks. However, to compare the two new models between themselves, STOASEP is better at getting higher hits, lower false alarms, higher correct nulls, lower misses than STSEP because it combines the criteria of both STOA and STSEP by using information of  $M_a$  and SEP. Furthermore, the  $p$  values shown in column 11 of Table 1 suggest that we may have considerable confidence in the STOASEP model but lesser confidence in the STSEP and STOA models.

[21] Continuing to follow *McKenna-Lawlor et al.* [2006], we use the same set of forecast skill scores commonly used by meteorological community as follows (for the detailed definition, please refer to the work of *McKenna-Lawlor et al.* [2006]).

[22] 1. Prob. of detection, yes (POD<sub>y</sub>), proportion of events with shock detection that were correctly forecast

[23] 2. Prob. of detection, no (POD<sub>n</sub>), proportion of events without shock detection that were correctly forecast.

**Table 2.** Statistical Comparison of the Performances of STOA, STSEP, and STOASEP in Terms of Several Standard Meteorological Forecast Skill Scores Using the Same Events of Solar Cycle 23 Used in Table 1

	Cycle Max			Cycle Rise			Composite		
	STOA	STSEP	STOASEP	STOA	STSEP	STOASEP	STOA	STSEP	STOASEP
Probability of detection, yes (POD <sub>y</sub> )	0.76	0.55	0.64	0.77	0.52	0.68	0.77	0.54	0.66
Probability of detection, no (POD <sub>n</sub> )	0.37	0.64	0.64	0.47	0.54	0.67	0.41	0.60	0.65
False alarm ratio (FAR)	0.59	0.53	0.49	0.53	0.59	0.44	0.56	0.56	0.47
BIAS	1.86	1.17	1.26	1.63	1.26	1.22	1.75	1.21	1.24
Critical success index (CSI)	0.36	0.34	0.40	0.41	0.30	0.44	0.39	0.32	0.42
True skill statistic (TSS)	0.13	0.19	0.29	0.24	0.07	0.34	0.18	0.14	0.31
Heidke skill score (HSS)	0.11	0.19	0.27	0.21	0.06	0.33	0.15	0.13	0.30
Gilbert skill score (GSS)	0.06	0.10	0.16	0.12	0.03	0.20	0.08	0.07	0.17
Root mean square of $\Delta T$ (hours)	11.2	12.3	11.4	11.8	10.4	11.8	11.5	11.5	11.6
Success rate (SR)	0.51	0.61	0.64	0.58	0.54	0.67	0.54	0.58	0.66

[24] 3. False alarm ratio (FAR), proportion of events with shock forecast that without shock detection,

[25] 4. BIAS, ratio of number of events with shock forecast to that with shock detection.

[26] 5. Critical success index (CSI), prob. of detection, yes, proportion of events with hits that with either shock forecast or shock detection.

[27] 6. True skill score (TSS), measures the ability to discriminate between shocks with detection and without.

[28] 7. Heidke skill score (HSS), percent correct, corrected by those expected correct by chance.

[29] 8. Gilbert skill score (GSS), CSI corrected by number of hits expected by chance.

[30] Table 2 shows statistical comparison of the performance of STOA, STSEP, and STOASEP in terms of the above standard meteorological forecast skill scores using the same events of Solar Cycle 23 used in Table 1, i.e., 207 events during the maximum phase and 170 events during the rise phase and for the composite sample. This table shows that for the composite sample of events, the 3 models have similar RMS value. However, during the cycle max and cycle rise, the RMS values for STSEP are larger (12.3) hours and smaller (10.4) hours, respectively. As we discussed above, STOA tends to forecast more shocks than the other models. From Table 2 we can see that STOA gets higher POD<sub>y</sub> and BIAS (which is proportional to the number of total shocks forecasted) but lower POD<sub>n</sub> and higher FAR than the other two models for events during cycle max, cycle rise, and for composite samples. Although both STSEP and STOASEP tend to forecast fewer shocks than STOA, since STOASEP is better at getting hits (h) and correct nulls (cn) than STSEP, STOASEP gets higher POD<sub>y</sub> and POD<sub>n</sub> and lower FAR than STSEP. For all the other forecast skill scores, CSI, TSS, HSS, GSS, STOASEP performs better than STOA. Furthermore, except CSI, the scores TSS, HSS, GSS of STOASEP is about double of that of STOA.

## 5. Conclusion

[31] We have studied the possibility of using the detection of energetic (38–53 keV) electrons at L1 to improve the interplanetary shock forecast models used by the community. In this paper we use STOA as an example. By considering the detection of energetic particles at L1, we create two new models, STSEP and STOASEP, based on STOA. To determine if the shocks will arrive at 1 AU, STSEP and STOASEP need SEP measurement at L1 and, in addition, STOASEP

also needs the calculation of magnetoacoustic Mach number  $M_a$ . Furthermore, to calculate shocks transit times, both STSEP and STOASEP use the method of STOA. To calculate  $M_a$ , the initial coronal shock velocity, the piston driving time, and the location on the Sun of the flare are required. In addition to the above inputs, the background solar wind velocity is required. This is taken to be the solar wind velocity measured at 1 AU (or a default value, e.g., 400 km/s, if “real time” ones are not available).

[32] In this paper we use ACE/EPAM SEP data obtained during cycle max and cycle rise of Solar Cycle 23 to show that our new model STOASEP, using both criteria of  $M_a$  and SEP, forecasts SAT with higher success rate than STOA. In addition, STOASEP performs better in terms of standard meteorological forecast skill scores CSI, TSS, HSS, and GSS. Therefore we expect that with electron-SEP measurement we can generally improve models in forecast of SAT at L1.

[33] In order to predict SAT in real time with the above models we have to use real-time electron-SEP data, for example, level one data of ACE SIP data broadcasted online. However, in this paper, we used level two electron-SEP data instead. As one of our future tasks we will work on real-time SAT prediction with the help of real-time SEP data. To calculate the transport of SEP in interplanetary space we use the free motion of particles with certain delay considering particles scattering in magnetic fluctuations. However, in the future, as we better understand SEP’s transport mechanism and we have better initial input for solar events, we will be able to get the transport of SEP by solving the transport equation numerically [Parker, 1963, 1965; Skilling, 1971; Ng and Wong, 1979; Schlüter, 1985; Ruffolo, 1991; Kocharov et al., 1998; Qin et al., 2004, 2005, 2006; Zhang et al., 2009]. However, because it is difficult to solve SEP transport equation numerically in real time, we may use a database method following Feng et al. [2009]. With the database method we create a database of solutions of the SEP transport equation organized on a multidimensional grid of solar event inputs, in real time, we predict the SEP transport by looking up in the grid of the database according to the solar event inputs with interpolation. In addition, we will study the forecasting of SAT with the help of SEP measurements based on other models, e.g., ISPM and HAFv.2.

[34] **Acknowledgments.** The authors benefited from the ACE/EPAM data provided by the ACE Science Center. This work profited enormously from discussions with Zdenka Smith. The authors are grateful for the

constructive comments and suggestions of the referees. This work was supported partly by grants NNSFC 40674095, 40621003, and 40523006. [35] Zuyin Pu thanks Zdenka Smith and another reviewer for their assistance in evaluating this paper.

## References

- Dryer, M. (1996), Comments on the origins of coronal mass ejections, *Sol. Phys.*, *169*, 421–429.
- Dryer, M., and S. F. Smart (1984), Dynamical models of coronal transients and interplanetary disturbances, *Adv. Space Res.*, *4*, 291–301.
- Feng, X. S., and X. H. Zhao (2006), A new prediction method for the arrival time of interplanetary shocks, *Sol. Phys.*, *238*, 167–186, doi:10.1007/s11207-006-0185-3.
- Feng, X. S., Y. Zhang, W. Sun, M. Dryer, C. D. Fry, and C. S. Deehr (2009), A practical database method for predicting arrivals of average interplanetary shocks at Earth, *J. Geophys. Res.*, *114*, A01101, doi:10.1029/2008JA013499.
- Fry, C. D., W. Sun, C. S. Deehr, M. Dryer, Z. Smith, S.-I. Akasofu, M. Tokumaru, and M. Kojima (2001), Improvements to the HAF solar wind model for space weather predictions, *J. Geophys. Res.*, *106*(A10), 20,985–21,001.
- Fry, C. D., M. Dryer, Z. Smith, W. Sun, C. S. Deehr, and S.-I. Akasofu (2003), Forecasting solar wind structures and shock arrival times using an ensemble of models, *J. Geophys. Res.*, *108*(A2), 1070, doi:10.1029/2002JA009474.
- Gold, R. E., M. Krimigis, S. E. Hawkins, D. K. Haggerty, D. A. Lohr, E. Fiore, T. P. Armstrong, G. Holland, and L. J. Lanzerotti (1998), Electron, proton and alpha monitor on the Advanced Composition Explorer Spacecraft, *Space Sci. Rev.*, *86*, 541–562.
- Kocharov, L., R. Vainio, G. Kovaltsov, and J. Torsti (1998), Adiabatic deceleration of solar energetic particles as deduced from Monte Carlo simulations of interplanetary transport, *Sol. Phys.*, *182*, 195–215.
- Lam, H.-L. (2009), Enhancement of solar wind low-energy energetic particles as precursor of geomagnetic disturbance in operational geomagnetic forecast, *Adv. Space Res.*, *43*, 1299, doi:10.1016/j.asr.2009.01.010.
- Lewis, D., and M. Dryer (1987), Shock-time-of-arrival model (STOA-87), *Tech. Rep., NOAA/SEL Contract Rep. (Syst. Doc.) to U.S. Air Weather Serv.*, U.S. Air Force Air Weather Serv., Scott AFB, Ill.
- Manoharan, P. K., N. Gopalswamy, S. Yashiro, A. Lara, G. Michalek, and R. A. Howard (2004), Influence of coronal mass ejection interaction on propagation of interplanetary shocks, *J. Geophys. Res.*, *109*, A06109, doi:10.1029/2003JA010300.
- McKenna-Lawlor, S. M. P., M. Dryer, M. D. Kartalev, Z. Smith, C. D. Fry, W. Sun, C. S. Deehr, K. Kecskemeti, and K. Kudela (2006), Near real-time predictions of the arrival at Earth of flare-related shocks during Solar Cycle 23, *J. Geophys. Res.*, *111*, A11103, doi:10.1029/2005JA011162.
- Ng, C. K., and K. Y. Wong (1979), Focused interplanetary transport of approximately 1 MeV solar energetic protons through self-generated Alfvén waves, in *Proc. 16th Int. Cosmic Ray Conf. (Kyoto)*, vol. 5, p. 252, Inst. for Cosmic Ray Res., Univ. of Tokyo, Tokyo, Japan.
- Parker, E. N. (1963), *Interplanetary Dynamical Processes*, Interscience, New York.
- Parker, E. N. (1965), The passage of energetic charged particles through interplanetary space, *Planet. Space Sci.*, *13*, 9–49.
- Qin, G., M. Zhang, J. R. Dwyer, and H. K. Rassoul (2004), Interplanetary transport mechanisms of solar energetic particles, *Astrophys. J.*, *609*, 1076–1081.
- Qin, G., M. Zhang, J. R. Dwyer, H. K. Rassoul, and G. M. Mason (2005), The model dependence of solar energetic particle mean free paths under weak scattering, *Astrophys. J.*, *627*, 562–566.
- Qin, G., M. Zhang, and J. R. Dwyer (2006), Effect of adiabatic cooling on the fitted parallel mean free path of solar energetic particles, *J. Geophys. Res.*, *111*, A08101, doi:10.1029/2005JA011512.
- Ruffolo, D. (1991), Interplanetary transport of decay protons from solar flare neutrons, *Astrophys. J.*, *382*, 688–698.
- Schlüter, W. (1985), Transport of solar wind fluctuations: A turbulence approach, Ph.D. thesis, Univ. of Kiel, Germany.
- Schwenn, R., A. D. Lago, E. Huttunen, and W. D. Gonzalez (2005), The association of coronal mass ejections with their effects near the Earth, *Ann. Geophys.*, *23*, 1033–1059.
- Skilling, J. (1971), Cosmic rays in the galaxy: Convection or diffusion?, *Astrophys. J.*, *170*, 265–273.
- Smart, D. F., and M. A. Shea (1985), A simplified model for timing the arrival of solar flare-initiated shocks, *J. Geophys. Res.*, *90*(A1), 183–190.
- Smart, D. F., M. A. Shea, W. R. Barron, and M. Dryer (1984), A simplified technique for estimating the arrival time of solar flare-initiated shocks, in *STIP Workshop on Solar/Interplanetary Intervals, 4–6 August 1982, Maynooth, Ireland*, edited by M. A. Shea et al., pp. 139–156, Bookcrafters, Inc., Chelsea, Mich.
- Smart, D. F., M. A. Shea, M. Dryer, A. Quintana, L. C. Gentile, and A. A. Bathurst (1986), Estimating the arrival time of solar flare-initiated shocks by considering them to be blast waves riding over the solar wind, in *Proceedings of the Symposium on Solar-Terrestrial Predictions*, edited by G. R. H. P. Simon and M. A. Shea, pp. 471–481, U.S. Gov. Print. Off., Washington, D. C.
- Smith, Z., and M. Dryer (1990), MHD study of temporal and spatial evolution of simulated interplanetary shocks in the ecliptic plane within 1 AU, *Sol. Phys.*, *129*, 387–405.
- Smith, Z., and R. Zwickl (1999), Forecasting geomagnetic storms using energetic particle enhancements, in *Solar Wind Nine*, edited by S. R. Habbal et al., *AIP Conf. Proc.*, *471*, 577–580.
- Smith, Z., M. Dryer, E. Ort, and W. Murtagh (2000), Performance of interplanetary shock prediction models STOA and ISPM, *J. Atmos. Terr. Phys.*, *62*, 1265–1274.
- Smith, Z., T. R. Detman, M. Dryer, C. D. Fry, C. C. Wu, and W. Sun (2004a), A verification method for space weather forecasting models using solar data to predict arrivals of interplanetary shocks at Earth, *IEEE Trans. Plasma Sci.*, *32*(4), 1498–1505, doi:10.1109/TPS.2004.832509.
- Smith, Z., W. Murtagh, and C. Smithtro (2004b), Relationship between solar wind low-energy energetic ion enhancements and large geomagnetic storms, *J. Geophys. Res.*, *109*, A01110, doi:10.1029/2003JA010044.
- Smith, Z. K., M. Dryer, S. M. P. McKenna-Lawlor, C. D. Fry, C. S. Deehr, and W. Sun (2009), Operational validation of HAFv2's predictions of interplanetary shock arrivals at Earth: Declining phase of Solar Cycle 23, *J. Geophys. Res.*, *114*, A05106, doi:10.1029/2008JA013836.
- Zhang, M., G. Qin, and H. Rassoul (2009), Propagation of solar energetic particles in 3-dimensional interplanetary magnetic fields, *Astrophys. J.*, *692*, 109–132.
- Zhao, X., X. Feng, and C.-C. Wu (2007), Influence of solar flare location and heliospheric current sheet on the associated shock arrival at Earth, *J. Geophys. Res.*, *112*, A06107, doi:10.1029/2006JA012205.

G. Qin, State Key Laboratory of Space Weather, Center for Space Science and Applied Research, Chinese Academy of Sciences, P.O. Box 8701, Beijing 100190, China. (gqin@spaceweather.ac.cn)

H. K. Rassoul and M. Zhang, Department of Physics and Space Sciences, Florida Institute of Technology, 150 West University Boulevard, Melbourne, FL 32901, USA. (rassoul@fit.edu; mzhang@fit.edu)